Dyes and Pigments 95 (2012) 296–303

Contents lists available at SciVerse ScienceDirect

Dyes and Pigments

journal homepage: www.elsevier.com/locate/dyepig

# Synthesis, photophysical and cytotoxicity evaluation of $A_3B$ type mesoporphyrinic compounds

Luís F. Vieira Ferreira [a,*], Diana P. Ferreira [a], Anabela S. Oliveira [a,b], Rica Boscencu [c,**], Radu Socoteanu [d], Mihaela Ilie [c], Carolina Constantin [e], Monica Neagu [e]

[a] Centro de Química-Física Molecular, Institute of Nanosciences and Nanotechnology, Instituto Superior Técnico, Av. Rovisco Pais, 1049-001 Lisboa, Portugal
[b] Escola Superior de Tecnologia e Gestão de Portalegre, Instituto Politécnico de Portalegre, Lugar da Abadessa, Apartado 148, 7300-901 Portalegre, Portugal
[c] Faculty of Pharmacy, "Carol Davila" University of Medicine and Pharmacy, 6 Traian Vuia St., 020956 Bucharest, Romania
[d] "Ilie Murgulescu" Institute of Physical Chemistry, Romanian Academy, 202 Splaiul Independentei, 060021 Bucharest, Romania
[e] "Victor Babeş" National Institute for Pathology and Biomedical Sciences, 99-101 Splaiul Independentei, 050096 Bucharest, Romania

ARTICLE INFO

*Article history:*
Received 6 March 2012
Received in revised form
11 May 2012
Accepted 14 May 2012
Available online 23 May 2012

*Keywords:*
Unsymmetrical mesoporphyrins
Singlet oxygen
Fluorescence
Cytotoxicity

ABSTRACT

A series of some $A_3B$ type mesoporphyrinic compounds were synthesized with superior yields using the microwave irradiation. The prepared compounds were characterized by elemental analysis, FT-IR, UV–Vis, NMR and EPR spectroscopy, which fully confirmed their structures. The spectral molecular absorption properties of the porphyrinic compounds were studied in different solvents and the influence of the solvent polarity on the absorbance maxima was described. Fluorescence emission and singlet oxygen formation quantum yields were evaluated for $A_3B$ type mesoporphyrinic compounds and compared with the corresponding symmetrical compounds, revealing high yields for the metal free compounds, followed by the zinc derivatives. The copper mesoporphyrinic compounds are not emissive and only evidence residual capacity for singlet oxygen formation. In order to establish their future potential in biomedical application preliminary toxicological studies, consisting of viability and proliferation of living cells in the presence of the unsymmetrical mesoporphyrinic compounds, were performed in the dark, on a standard cell line of human Caucasian histiocytic lymphoma (U937). The obtained results indicate a very low or no cytotoxicity at all for all compounds under study. Therefore further testing with light activation protocols is recommended in future work.



## 1. Introduction

In the last decades a great interest was directed towards fluorescence probes, having structures that mimic naturally occurring compounds. Porphyrins, due to their unique photophysical and photochemical properties, can easily be turned into promising candidates to be used both as fluorescent markers and as agents for photodynamic therapy [1–13]. The ideal molecule to be used as sensitizer or marker should have convenient emission in the phototherapeutic window (~600–900 nm) [1,3,4,7], high quantum yield of singlet oxygen generation, relatively high fluorescence lifetime and low level of dark toxicity. The subcellular localization of porphyrins plays a major role in their biomedical efficiency. The cellular affinity of a porphyrinic compound is governed by its amphiphilic character, which depends on the regiochemical arrangement of hydrophobic and hydrophilic meso-substituents in the structure. That is why our research was directed towards obtaining novel mesoporphyrinic compounds, simultaneously being amphiphilic and having suitable physical–chemical properties [14–18]. This paper presents the synthesis of some $A_3B$ type mesoporphyrinic compounds: 5-(2-hydroxyphenyl)-10,15,20–tris(4-carboxymethylphenyl) porphyrin ($TCMPOH_O$), Cu(II)-5-(2-hydroxyphenyl)-10,15,20–tris(4-carboxymethylphenyl) porphyrin ($Cu(II)TCMPOH_O$) and Zn(II)-5-(2-hydroxyphenyl)-10,15,20–tris(4-carboxymethylphenyl) porphyrin ($Zn(II)TCMPOH_O$) (Scheme 1), using microwave irradiation assisted synthesis.

Before being investigated in connection with their effect on living cells and/or tissues, the novel compounds need to be properly characterized, namely in what respects their physical-chemical properties, including the determination of its photophysical parameters [19–27]. Therefore, the study of the ground state absorption, fluorescence emission (quantum yields and lifetimes) and singlet oxygen generation quantum yields was performed for all compounds

* Corresponding author. Tel.: +351 21 84 19 252; fax: +351 21 846 44 55.
** Corresponding author.
*E-mail addresses:* luisfilipevf@ist.utl.pt (L.F. Vieira Ferreira), diana.ferreira@ist.utl.pt (D.P. Ferreira), asoliveira@ist.utl.pt (A.S. Oliveira), rboscencu@yahoo.com (R. Boscencu), psradu@yahoo.com (R. Socoteanu), m16ilie@yahoo.com (M. Ilie), caroconstantin@yahoo.com (C. Constantin), neagu.monica@gmail.com (M. Neagu).

0143-7208/$ – see front matter © 2012 Elsevier Ltd. All rights reserved.
doi:10.1016/j.dyepig.2012.05.012

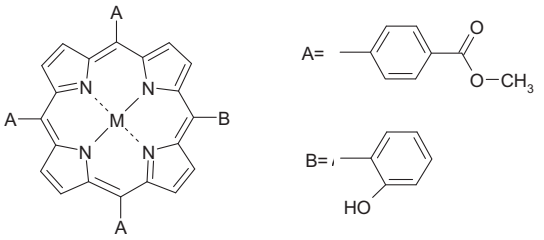


| | |
|---|---|
| **TCMPOHo** | M=2H |
| **M(II)TCMPOHo** | M= Zn(II), Cu(II) |
| **TCMP** | **B=A**, M=2H |
| **M(II)TCMP** | **B=A**, M= Zn(II), Cu(II) |

**Scheme 1.** Structures of the unsymmetrical ($A_3B$ type) and symmetrical ($A_4$) mesoporphyrinic compounds used in this study.

synthesized and for the corresponding symmetrical compounds, 5,10,15,20-mesotetrakis(4-carboxymethylphenyl) porphyrin (TCMP) and M(II)-5,10,15,20-mesotetrakis(4-carboxymethylphenyl) (M(II) TCMP) in order to be compared. Also, the $A_3B$ type mesoporphyrinic compounds were evaluated in terms of their cytotoxicity.

## 2. Experimental

### 2.1. Materials and equipment

Commercially available chemicals and solvents were used as received from Sigma–Aldrich and Merck. For the microwave assisted synthesis we used a Clatronic MWG775H type temperature-controlled microwave oven. The elemental analysis of C, H and N was performed with an automatic Carlo Erba 1108 analyzer. IR spectra were recorded with an FT-IR 400D Nicolet Impact spectrophotometer. The substances under analysis, previously dried for 24 h at 150 °C, were processed as KBr pellets of spectroscopic purity. The spectra were recorded within the range 4000–500 $cm^{-1}$. The absorption spectra were recorded with a Camspec M501 single beam scanning UV/Visible spectrophotometer at room temperature and in the spectral range of 200–1100 nm. The porphyrin solutions were freshly prepared in the spectrally pure solvents at the concentration $2.5 \times 10^{-6}$ M and kept in dark until the measurement to prevent photodegradation. The NMR spectra were recorded with a 400 MHz Bruker NMR Spectrometer. EPR spectra of the copper complex were recorded using an ART-6 spectrometer, operating in the X band (9.01 GHz), equipped with a 100 kHz field modulation unit.

### 2.2. Synthesis of $A_3B$ type mesoporphyrinic compounds

#### 2.2.1. Synthesis of 5-(2-hydroxyphenyl)-10,15,20–tris(4-carboxymethylphenyl) porphyrin ($TCMPOH_O$)

Methyl 4-formylbenzoate (4.92 g, 0.03 mol), redistilled 2-hydroxybenzaldehyde (1.04 mL, 0.01 mol), fresh distilled pyrrole (2.76 mL, 0.04 mol) and 4–5 g of Silica gel 60 (200–500 μm, 35–70 mesh) were mixed at room temperature in a Pyrex bottle. The mixture reaction was subsequently subjected to microwave irradiation for 10 min at 170 °C and 450 W. The extraction of the samples for synthesis monitoring was performed every 2 min during the irradiation, and the presence of the porphyrinic compounds in the sample was assessed by thin layer chromatography and UV–Vis spectroscopy. Thin layer chromatography (dichloromethane/diethyl ether 50:1 v/v) of the crude product revealed presence of a mixture six isomers ($A_4$, $A_3B$, $A_2B_2$(*cis* and *trans*), $AB_3$ and $B_4$–type) with high percent of the 5-(2-hydroxyphenyl)-10,15,20–tris(4-carboxymethylphenyl) porphyrin ($A_3B$ isomer). Upon reaction completion, the final product was dissolved in dichloromethane/diethyl ether (50:1, v/v) and filtered in order to further purify the mesoporphyrinic compounds. The solvent was removed under reduced pressure and the crude product was purified by repeated column chromatography elution, using dichloromethane/diethyl ether (50:1, v/v) as eluent and silica gel (100–200 mesh size) as stationary phase. $A_3B$ isomer was the second band that passes through the chromatographic column, the first band containing $A_4$ isomer (5,10,15,20-mesotetrakis(4-carboxymethylphenyl) porphyrin). In order to comparative evaluation the first two isomers were separed and characterized. The final mesoporphyrinic compounds was obtained by preparative TLC (2 mm Silica gel 60 plates were used). The obtained yield was 33% for $A_3B$ isomer and 48% for $A_4$ isomer. For 5, 10, 15, 20-mesotetrakis-(4-carboxymethylphenyl) porphyrin analitical data was identical with those prevously reported [28]. Elemental analysis for $C_{50}H_{36}N_4O_7$: calculated C 74.62, H 4.47, N 6.96; found C 74.44, H 4.35, N 6.78. The chemical shifts of the NMR signals for the $TCMPOH_O$ are as follows: $^1$H-NMR (400 MHz, $CDCl_3$), $\delta_H$ ppm -2.75 (s, 2H), 4.15 (s, 9H), 5.12 (s, 1H), 7.08 (m, 1H), 7.37 (m, 1H), 7.42 (m, 1H), 7.75 (m, 1H), 8.32 (d, $J = 8.0$ Hz, 6H), 8.48 (d, $J = 8.0$ Hz, 6H), 8.86 (d, $J = 4.7$ Hz, 6H), 8.95 (d, $J = 4.7$ Hz, 2H).

$^{13}$C-NMR (400 MHz, $CDCl_3$), $\delta_C$ ppm 53.2, 66.9, 114.8, 120.2, 121.0, 121.9, 128.2, 134.5, 135.4, 145.0, 146.9, 150.9. IR (KBr): 3413, 3314, 2920, 2850, 1717, 1606, 1495, 1434, 1273, 1102, 982, 866, 798, 758. UV–Vis ($\lambda_{max}$ (nm)) in $CH_2Cl_2$: 419.1, 514.6, 549.1, 589.2, 646.1.

#### 2.2.2. Synthesis of M(II)-5-(2-hydroxyphenyl)-10,15,20–tris(4-carboxymethylphenyl) porphyrin [M(II) $TCMPOH_O$, M = Zn, Cu]

2-hydroxybenzaldehyde freshly distilled (1.04 mL, 0.01 mol), methyl 4-formyl benzoate (4.92 g, 0.03 mol), freshly distilled pyrrole (2.76 mL, 0.04moli), anhydrous copper chloride (1.344 g, 0.01 mol), and 4–5 g of Silica gel 60 (200–500 μm, 35–70 mesh) in the presence of 2,6-dimethylpyridine (1 mL) were irradiated in a Pyrex bottle by a microwave oven at 180 °C, 475 W for 10 min. The extent of the complexation reaction was monitored by TLC and UV–Vis spectroscopy. TLC analysis on silica gel, using a dichloromethane/diethyl ether mixture as eluent, allowed us to identify a number of six isomeric metalloporfirins ($A_4$, $A_3B$, $A_2B_2$(*cis* and *trans*), $AB_3$ and $B_4$–type) in the final reaction mixture.

In order to separate compounds of interest, the crude product was first dissolved in dichloromethane/diethyl ether (50:1 v/v), then filtered and finally purified by column chromatography, repeated elution, using silica gel (100–200 mesh size) as stationary phase and dichloromethane/diethyl ether (50:1, v/v) as eluent. The first two metalloporphyrinic isomers ($A_4$ and $A_3B$ type) were separed for this study. The solution of the porphyrinic complexes was concentrated under reduced pressure and the obtained violet crystals were dried at ≈100 °C for 12 h. The obtained yields were 40% for Cu(II)$TCMPOH_O$.

The preparation of the Zn(II)$TCMPOH_O$ was similar to that of Cu(II)$TCMPOH_O$, using anhydrous zinc chloride. Zn(II)-5-(2-hydroxyphenyl)-10,15,20–tris(4-carboxymethylphenyl) porphyrin was obtained with a yield of 38%. Zn(II)TCMP and Cu(II)TCMP were obtaining with a yields about 55% and physico-chemical characteristics was identical with those prevously reported [14,15].

Elemental analysis for $C_{50}H_{34}N_4O_7Zn$: calculated C 69.21, H 3.92, N 6.45; found C 69.06, H 3.84, N 6.31. The chemical shifts and the multiplicities of the $^1$H-NMR signals for the Zn(II)$TCMPOH_O$, besides important adjacent data provided by $^{13}$C-NMR, are as follows: $^1$H-NMR (400 MHz, $CDCl_3$), $\delta_H$ ppm 4.14 (s, 9H), 5.12 (s, 1H), 7.08 (m, 1H), 7.37 (m, 1H), 7.42 (m, 1H), 7.75 (m, 1H), 8.32 (d, $J = 8.0$ Hz, 6H), 8.48 (d, $J = 8.0$ Hz, 6H), 8.86 (d, $J = 4.7$ Hz, 6H), 8.95

(d, $J = 4.7$ Hz, 2H). $^{13}$C-NMR (400 MHz, $CDCl_3$), $\delta_C$ ppm: 53.3, 114.8, 120.3, 121.1, 121.9, 128.2, 134.5, 135.5, 145.0, 147.0, 150.9.

IR (KBr): 3414, 2921, 2851, 1720, 1606, 1486, 1435, 1273, 1101, 995, 867, 794, 762. UV–Vis ($\lambda_{max}$ (nm)) in $CH_2Cl_2$: 420.6, 548.2, 586.0.

Elemental analysis for $C_{50}H_{34}N_4O_7Cu$: calculated C 69.32, H 3.93, N 6.47; found C 69.22, H 3.80, N 6.36. IR (KBr): 3414, 2921, 2852, 1720, 1608, 1486, 1435, 1274, 1102, 999, 867, 797. UV–Vis ($\lambda_{max}$ (nm)) in $CH_2Cl_2$: 416.0, 539.8. The EPR parameters evaluated for the Cu(II)TCMPOH$_O$ are: $g_{||} = 2.172$, $g_{\perp} = 2.050$, $A_{||} = 202 \times 10^{-4}$ cm$^{-1}$, $A_{\perp} = 30 \times 10^{-4}$ cm$^{-1}$.

### 2.3. Dark cytotoxicity tests

The preliminary toxicological studies in the presence of the unsymmetrical mesoporphyrinic compounds consisted in viability and proliferation studies performed on the standard cell line of human Caucasian histiocytic lymphoma U937.

#### 2.3.1. Cell line and culture conditions

U937 cell line was purchased from ECACC (catalog no. 85011440) and cultured in RPMI 1640 medium supplemented with 100U/mL penicillin, 0.1 mg/mL streptomycin, 0.25 μg/mL amphotericin, 2 mM glutamine and 10% fetal bovine serum. The cells were maintained at 37 °C in a 5% $CO_2$ humid atmosphere for standard cultivation and during all the toxicological tests.

#### 2.3.2. Sample preparation

The mesoporphyrinic compounds solutions were handled in sterile conditions. 10 mM stock solutions of the compounds to be tested were prepared in DMSO by sonication at 22000 Hz for 30 s. For the toxicological tests the solutions were further diluted in RPMI 1640 culture medium for the toxicological tests in the range 1.25–40 μM. For the viability and the proliferation test assay, the cells (cell density $5 \times 10^{-4}$ cells/mL) were incubated with each of the tested concentrations for 2, 24 and 48 h. A cellular control consisting in unloaded/untreated U937 cells was used for every replicate of the tests, corresponding to each incubation time.

#### 2.3.3. Viability and proliferation assays

For cellular viability we have used lactate dehydrogenase (LDH) release test [29], using CytoTox 96® Non-Radioactive Cytotoxicity Test (Promega). For testing cell proliferation by means of the tetrazolium salt (MTS) reduction test [30], we have used CellTiter 96® AQeous One Solution Cell Proliferation Assay kit (Promega). Briefly, at end of each incubation time with the mesoporphyrinic complexes, the cell supernatants were collected for LDH test whilst the cell sediment was used for MTS assay. Results were expressed as triplicate's mean of optical density (OD) ± SD.

### 2.4. Fluorescence lifetime determinations

Fluorescence lifetimes were determined using Easylife V™ equipment from OBB (Lifetime range from 100 ps to 3 μs). This technique uses pulsed light sources from different LEDs (310 nm in this case) and measures fluorescence intensity at different time delays after the excitation pulse. In this case, 590 nm cut-off filters were used at emission both for solution and for solid samples, depending on the sample under study. The instrument response function was measured using a Ludox scattering solution. FelixGX software from OBB was used for fitting and analysis of the decay dynamics, 1 to 4 exponentials and also a lifetime distribution analysis [31], the Exponential Series Method (ESM).

### 2.5. Laser-induced luminescence (LIL)

The schematic diagram of the LIL system is presented in reference [32]. A $N_2$ laser (PTI model 2000, *ca.* 600 ps FWHM, ~1.0 mJ per pulse), was used in laser-induced luminescence experiments. In this case the excitation wavelength was 337 nm. The light arising from the irradiation of the samples by the laser pulse was collected by a collimating beam probe coupled to an optical fibre (fused silica) and detected by a gated intensified charge coupled device Andor ICCD, model i-Star 720. The ICCD was coupled to a fixed compact imaging spectrograph (Andor, model Shamrock 163). The system can be used either by capturing all light emitted by the sample or in a time-resolved mode. The ICCD has high speed gating electronics (about 2.3 ns) and intensifier and cover at least the 250–950 nm wavelength range. Time-resolved absorption and emission spectra are available in a time range from nanoseconds to seconds. With this set-up, both fluorescence and phosphorescence spectra were easily available by the use of the variable time gate width and start delay facilities of the ICCD.

### 2.6. Quantum yield of singlet oxygen determinations

The singlet oxygen measurement set-up was assembled in our laboratory. As an excitation source we use the nitrogen laser as described in 2.5. The detector is an InGaAs CCD (model i-Dus from Andor) working at low temperature (−60 °C) coupled to a fixed spectrograph, model Shamrock 163i also from Andor. Long pass filters were used to totally exclude the excitation radiation from reaching the detector (LFP1000 or LFP1100 from CVI Lasers).

## 3. Results and discussion

### 3.1. Chemistry

All the reactions in this paper have been successfully repeated several times with identical results and the physical chemical features for all mesoporphyrinic compounds are identical. All the newly synthesized compounds are soluble in organic solvents such as: ethanol, *iso*-propanol, dimethylsulfoxide, chloroform, dimethylformamide and dichloromethane.

$^1$H-NMR spectrum of the TCMPOH$_O$ shows the single peak at about −2.75 ppm which confirm the presence of the −NH group in porphyrinic core. The comparative study of $^1$H-NMR data of asymmetrical mesoporphyrinic ligand and its zinc complex reveals the absence of this signal, indicating the involvement of both nitrogen atoms of porphyrinic ring in the coordination after deprotonation. The remained $^1$H-NMR signals are displayed with perfect equivalence for the TCMPOH$_O$ and Zn(II)TCMPOH$_O$, proving, as expected, that the influence of the central metal ion is restrained to the core, with no influence on the peripheral substituents. Instead, the asymmetry of those substituents exercise an obvious influence on the β pyrrolic positions, due to the 400 MHz NMR capacity, segregating the signals in two categories, for the positions 2,18 − $\delta$ value is 8.95 ppm and for the positions 3,7,8,12,13,17 − $\delta$ is 8.86 ppm, respectively. The strong peripheral asymmetry is revealed also by the different free positions in the benzene substituted rings, and by the signals for the proton of the −OH group at 5.12 ppm *vs*. the 9 protons for three $-COOCH_3$ groups at 4.15 ppm.

IR spectrum of TCMPOH$_O$ shows a medium band at 3314 cm$^{-1}$ assigned to the N–H stretching vibration of the porphyrinic core, which disappears on complexation and could be due to the coordination of both nitrogen atoms of the porphyrinic core to the metal centers. The presence of the −OH functional group in the structure of

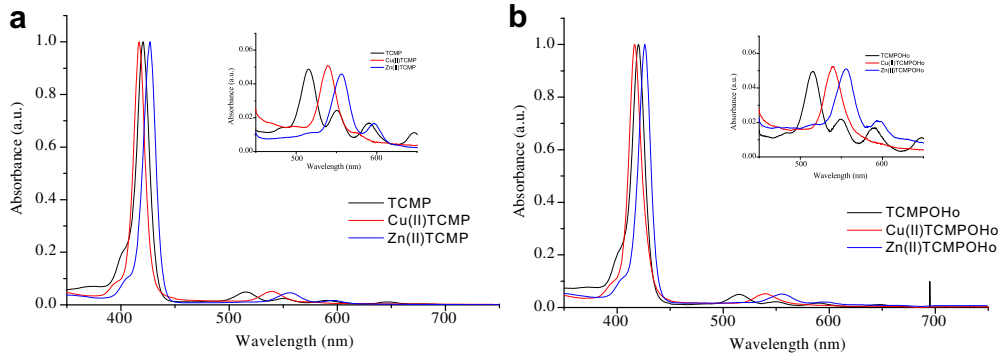


**Fig. 1.** Ground state absorption spectra of a) $TCMPOH_O$, b) Cu(II)$TCMPOH_O$ and c) Zn(II)$TCMPOH_O$ in chloroform.

the compounds $TCMPOH_O$, Zn(II)$TCMPOH_O$ and Cu(II)$TCMPOH_O$ is responsible for the appearance of a large band at about 3414 $cm^{-1}$ assigned to O–H stretching vibration. The IR spectrum of the asymmetric porphyrinic compounds clearly indicates the presence of the -O-$CH_3$ group in the spectral range 2850–2852 $cm^{-1}$. The bands of the compounds in the spectral range of 1717–1720 $cm^{-1}$ are assigned to C=O stretching vibration. In addition, in the IR spectra of the asymmetric porphyrinic compounds the strong absorption band at about 1274 $cm^{-1}$ can be attributed to the C–O groups. Other bands observed in the higher wavenumber region (~2920 $cm^{-1}$) are due to the stretching vibrational motion of C–H bond of the porphyrin ring. Also, the band at about 1435 $cm^{-1}$ includes the C–H stretching of the pyrrole rings and the bands at ~1608 $cm^{-1}$ and 1486–1495 $cm^{-1}$ can be assigned to C–N stretching vibrations.

EPR spectra of the Cu(II)TCMPOHo was recorded on powders at room temperature. The spectroscopic values obtained by EPR spectra of the copper asymmetrical mesoporphyrinic complex are close to those presented in the literature and are characteristic for Cu(II) in square planar surroundings with $D_{4h}$ symmetry [33,34]. In fact, in order to get the Cu(II) inclusion in ligand two protons bonded to nitrogens have to be removed from the inner part of the porphyrinic ligand, leading to complexes with higher symmetry of the coordination geometry (from $D_{2h}$ for the metal free ligands to $D_{4h}$ for any of the Cu(II) complex). Also, the $g_{||}$ value ($g_{||} < 2.3$) indicates a covalent character of the Cu–N bonds in the Cu(II) TCMPOHo [35].

### 3.2. Photochemical characterization

#### 3.2.1. Ground state UV–Visible spectral characterization

Ground state absorption spectra of all dyes in chloroform are presented in Fig. 1.

The maximum wavelengths and molar absorptivity of the asymmetrical mesoporphyrinic compounds synthesized in this work are presented in Table 1.

The electronic absorption spectrum of the $TCMPOH_O$ display a typical Soret band, peaking at 415–421 nm, followed by the four Q-bands located in the spectral range of 512–648 nm, depending on the solvent. The decrease in the number of Q bands in the UV–Vis absorption spectra of the porphyrinic complexes studied in this paper is the consequence of the metal ion inclusion in the free base ligand. Thus, the molecular electronic spectra of Zn(II) $TCMPOH_O$, exhibited one Soret band in the spectral range of 423–431 nm accompanied by two Q bands, respectively in the 556–562 nm and 597–602 nm spectral range. The copper porphyrinic complexes shows a Soret band in the 413–421 nm region and a single Q band in the spectral range of 538–544 nm.

**Table 1**
Maximum wavelength and molar absorptivity of the porphyrinic compounds in different solvents ($c = 2.5 \times 10^{-6}$ M).

| Solvent | $\lambda_{max}$ (nm) [log$\varepsilon$ (L $mol^{-1}$ $cm^{-1}$)] | | | | |
|---|---|---|---|---|---|
| | Soret B(0,0) | Q*y* (1,0) | Q*y* (0,0) | Q*x* (1,0) | Q*x* (0,0) |
| *5-(2-hydroxyphenyl)-10,15,20–tris(4-carboxymethylphenyl) porphyrin* | | | | | |
| EtOH | 416.6 [5.562] | 513.2 [4.237] | 547.0 [3.889] | 588.9 [3.720] | 647.0 [3.574] |
| *i*-PrOH | 418.0 [5.594] | 513.9 [4.261] | 548.0 [3.884] | 589.2 [3.740] | 647.8 [3.574] |
| $CHCl_3$ | 420.1 [5.445] | 514.1 [4.151] | 549.0 [3.793] | 589.2 [3.785] | 648.6 [3.556] |
| $CH_2Cl_2$ | 419.1 [5.658] | 514.6 [4.306] | 549.1 [3.903] | 589.2 [3.796] | 646.1 [3.628] |
| DMF | 419.4 [5.628] | 514.6 [4.290] | 549.0 [3.916] | 590.0 [3.740] | 646.6 [3.677] |
| DMSO | 420.8 [5.613] | 515.4 [4.267] | 549.4 [3.889] | 590.0 [3.720] | 646.7 [3.628] |
| *Zn(II)-5-(2-hydroxyphenyl)-10,15,20–tris(4-carboxymethylphenyl) porphyrin* | | | | | |
| EtOH | 425.0 [5.631] | – | 557.5 [4.169] | 598.0 [3.593] | – |
| *i*-PrOH | 426.1 [5.613] | – | 557.8 [4.218] | 598.0 [3.726] | – |
| $CHCl_3$ | 426.0 [5.627] | | 555.5 [4.191] | 592.5 [3.910] | |
| $CH_2Cl_2$ | 420.6 [5.602] | – | 548.2 [4.251] | 586.0 [3.542] | – |
| DMF | 428.0 [5.603] | – | 559.7 [4.170] | 600.0 [3.781] | – |
| DMSO | 430.5 [5.608] | – | 561.1 [4.225] | 601.8 [3.903] | – |
| *Cu(II)-5-(2-hydroxyphenyl)-10,15,20–tris(4-carboxymethylphenyl) porphyrin* | | | | | |
| EtOH | 413.4 [5.665] | – | 537.5 [4.274] | – | – |
| *i*-PrOH | 414.5 [5.662] | – | 538.0 [4.328] | – | – |
| $CHCl_3$ | 416.5 [5.676] | | 540.5 [4.284] | | |
| $CH_2Cl_2$ | 416.0 [5.593] | – | 539.8 [4.244] | – | – |
| DMF | 417.0 [5.633] | – | 539.7 [4.310] | – | – |
| DMSO | 420.8 [5.582] | – | 543.3 [4.326] | – | – |

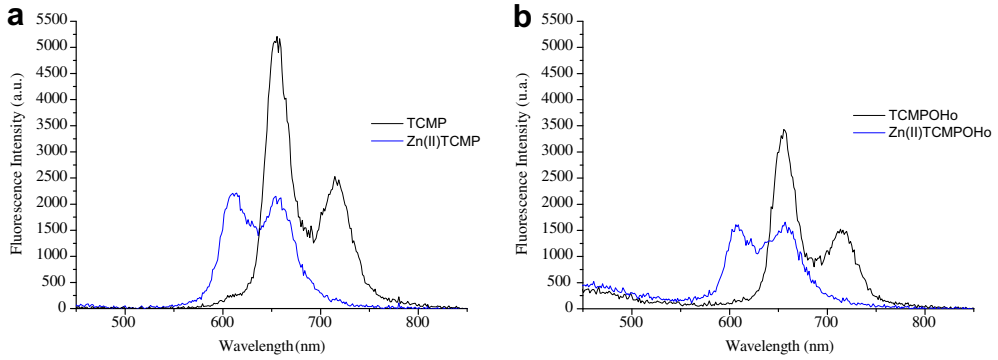


**Fig. 2.** Fluorescence emission spectra of a) $TCMPOH_O$ and b) Zn(II)$TCMPOH_O$ in chloroform.

According to Gouterman's theory [36], the Soret band is result of $a_{1u}$ ($\pi$) → $e_g$ ($\pi^*$) transition and Q bands corresponding to the $a_{2u}$ ($\pi$) → $e_g$ ($\pi^*$) transition. Comparing the UV–Vis spectra corresponding to the zinc porphyrinic complexes *versus* copper porphyrinic complexes (as can be seen in Table 1) the blue shift of the spectral bands of the copper complex was evidenced. In agreement with Gouterman's theory, this blue shift of the Soret and Q bands could originate from the stronger conjugation effects that occur between the Cu(II) orbitals and the $\pi$ electrons of the tetrapyrrolic ring, effects that cause a decrease the energy of the $a_{1u}$ ($\pi$) and $a_{2u}$ ($\pi$) orbitals relative to the $e_g$ ($\pi^*$) orbitals with increased the energy available for electron transitions [36].

The analysis of spectral data obtained from UV–Vis spectra of the porphyrinic compounds studied in this paper reveals changes in the relative positions of the Soret band and the Q bands, depending on the solvent polarity. Thus, in the case of the $TCMPOH_O$, the Soret band is bathochromically shifted by about 5 nm, while for the corresponding complexes with cooper and zinc this shift is larger (about 7 nm), with decreasing solvent polarity. The changes in Soret and Q bands can be associated with the solvent polarity and reflects the physical interaction between the porphyrinic substituents and the solvent molecule. The spectral changes that appear for the compounds TCMPOHo, Zn(II) TCMPOHo, Cu(II)TCMPOHo diluted in protic solvents can be attributed to both the hyperconjugation effect of the hydroxyphenyl group (the asymmetry element) and the hydrogen bonds between the solvent molecules and the functional groups in the *meso* positions of the porphyrinic macrocycle.

### 3.2.2. Fluorescence emission spectra and fluorescence lifetime decays

Fig. 2 presents the laser induced fluorescence emission spectra of TCMP, Zn(II)TCMP, $TCMPOH_O$, and Zn(II)$TCMPOH_O$ in chloroform. By comparison with TPP [37] and ZnTPP as references, the fluorescence quantum yields ($\Phi_F$) were obtained in chloroform.

**Table 2**
Fluorescence emission quantum yields, singlet oxygen formation quantum yields and fluorescence lifetimes for the mesoporphyrinic under study.

| Compound | $\Phi_\Delta$ in $CHCl_3$ | $\Phi_F$ in $CHCl_3$ | Lifetime (ns) | $\chi 2$ |
|---|---|---|---|---|
| Phenazine | 0.84 | – | – | – |
| TPP | 0.40 | 0.11 | 9.5 | 1.09 |
| ZnTPP | 0.23 | 0.04 | 2.2 | 1.04 |
| TCMP | 0.49 | 0.11 | 9.2 | 1.06 |
| Cu(II)TCMP | 0.04 | 0 | 0 | 0 |
| Zn(II)TCMP | 0.43 | 0.06 | 1.9 | 1.16 |
| TCMPOHo | 0.39 | 0.07 | 9.2 | 1.14 |
| Cu(II)TCMPOHo | 0.12 | 0.004 | 2.0 | 0.94 |
| Zn(II)TCMPOHo | 0.27 | 0.03 | 2.0 | 1.39 |

As we can see in Table 2, we also determined the fluorescence lifetimes for all compounds in chloroform. Fig. 3 shows the lifetime decays of the porphyrins TCMPOHo and Zn(II)$TCMPOH_O$ as an example. A mono-exponential decay was observed for all dyes suggesting the existence of a single fluorescing species present in all cases. The trend exhibited by the fluorescence lifetimes (Table 2) is in reasonable agreement with the fluorescence quantum yields trend for all compounds under study.

### 3.2.3. Singlet oxygen quantum yields

To evaluate the photosensitizing efficacy of the porphyrins, the singlet oxygen formation quantum yields ($\Phi_\Delta$) were measured. Phenazine was used as the standard for the determination of the $\Phi_\Delta$ [38]. In Fig. 4 we can see the singlet oxygen emission spectra of some sensitizers used in this work (Fig. 5).

All these significative parameters, including singlet oxygen formation quantum yields four all the porphyrins under study are summarized in Table 2.

As Table 2 shows, Cu(II) inclusion in the porphyrin highly reduces the fluorescence emission. This effect is due to the copper presence which increases the non-radiative decay of the excited singlet state of the porphyrin [39], decreasing at the same time the quantum yield of singlet oxygen formation, which involves the triplet excited state of the porphyrin. Both metal free and zinc porphyrins are good singlet oxygen generators with quantum yield values ranging from 0.27 to 0.49 in chloroform. The TCMP porphyrin displayed the highest quantum yield compared to the other porphyrin derivatives. Metal free porphyrin exhibits a very reasonable fluorescence quantum yield of emission ($\Phi_F$ = 0.07 and 0.11) as well as a long lifetime ($\tau_F$ = 9.2 ns), which points to be used as a diagnostic tool for the detection of cancer cells [40].

## 3.3. Viability and proliferation in vitro tests

It is well known that photosensitizer agents tend to accumulate mainly in the tumor tissue in a higher extent relative to the surrounding health tissue and their fluorescing properties may be used for cancer detection [7,41]. To explore whether a chemical entity like a porphyrin structure could act as a tissue marker based on its fluorescence characteristics, the very first step is to establish the dark cytotoxicity profile of the compound. In order to achieve this essential step, the newly synthesized mesoporphyrinic compounds were tested following short and long-term incubation with U937 standard tumor cell line. The cellular viability and proliferative capacity were assessed upon each round of cell incubation with the novel porphyrins to evaluate the potential *per se* cytotoxicity of the compounds.

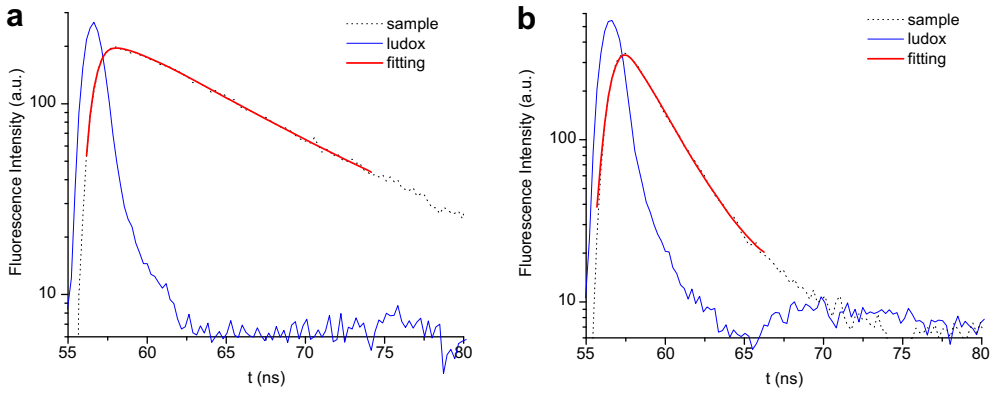


**Fig. 3.** Fluorescence lifetime decays of a) $TCMPOH_O$ and b) $Zn(II)TCMPOH_O$ in chloroform.

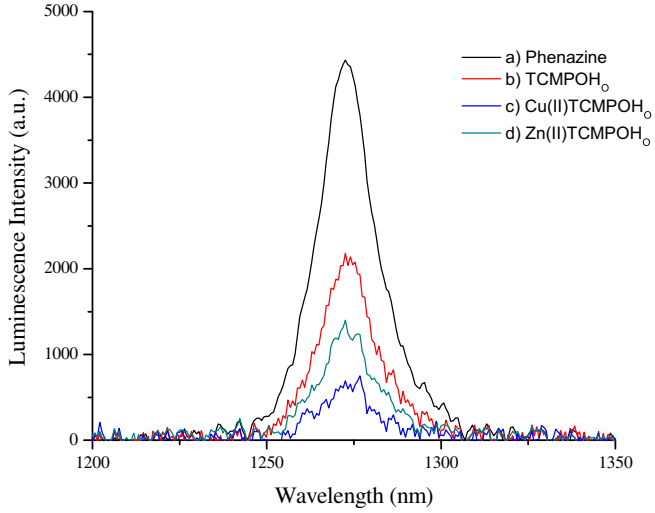


**Fig. 4.** Singlet oxygen emission spectra of: a) Phenazine and b)$TCMPOH_O$, c) Cu(II) $TCMPOH_O$ and d) $Zn(II)TCMPOH_O$ in chloroform.

### 3.3.1. *Short term cytotoxicity assessment*

A short time incubation system with a porphyrin as applicant for a photosensitizer is a prerequisite for its efficacy in tumor therapy when a new therapeutic compound is to be obtained or its use for an imagistic purpose is to be reached [42,43].

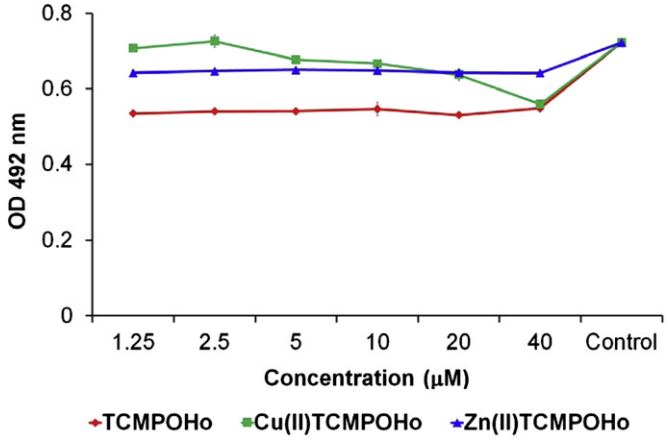


**Fig. 5.** The viability of U937 cells incubated 2 h with TCMPOHo compounds series; the LDH release registered as OD at 492 nm.

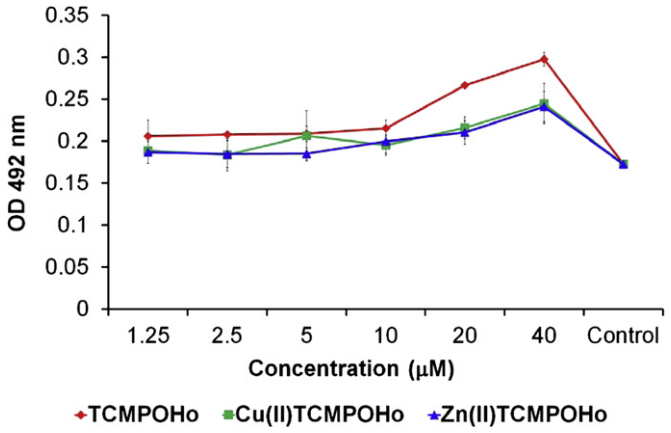


**Fig. 6.** The proliferation of U937 cells incubated 2 h with TCMPOHo compounds series; the MTS reduction reaction registered as OD at 492/620 nm.

Short term incubation (2 h) of U937 cells with all asymmetrical mesoporphyrinic compounds resulted in no major influence on the cellular viability in terms of LDH release, not even in high concentration (40 μM), as the level of LDH release was actually below the level of the control sample. Moreover, at short time incubation, the cell multiplication capacity is not affected by the porphyrinic compounds; we noticed even a slight stimulation of

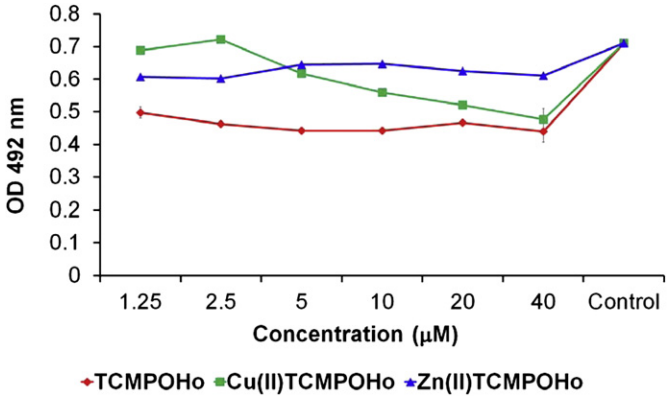


**Fig. 7.** The viability of U937 cells incubated 24 h with TCMPOHo compounds series; the LDH release registered as OD at 492 nm.

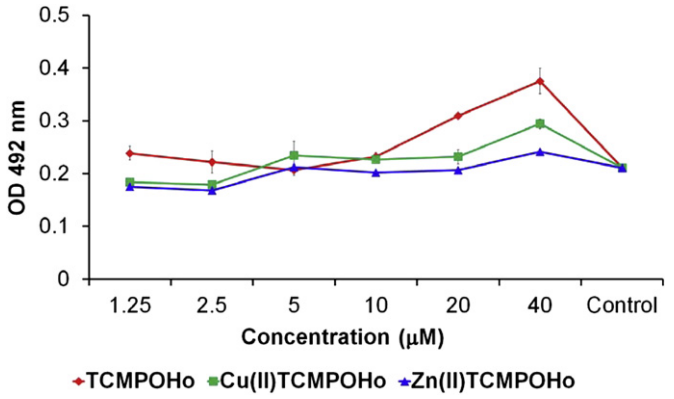


**Fig. 8.** The proliferation of U937 cells incubated 24 h with TCMPOHo compounds series; the MTS reduction reaction registered as OD at 492/620 nm.

proliferation at high doses (20–40 μM) for all the asymmetrical mesoporphyrinic compounds (Fig. 6).

*3.3.2. Long-term cytotoxicity evaluation*

A prolonged incubation with the mesoporphyrinic compounds "strikes twice" in giving an answer regarding whether there could be a possible delayed cytotoxicity developed upon cells if the photosensitizing aim is targeted or about their remanency in cellular structures if a detection mean is sought. The results indicate that the non-toxic properties of the newly mesoporphyrinic compounds upon U937 cell line is maintained following 24 and respectively 48h incubation; the MTS reduction tests performed by metabolically active cells seem to follow a similar curve for both series, with minor stimulation at high doses, mainly for $TCMPOH_o$ and a slender inhibition of the cell proliferation at low doses (1.25 and 2.5 μM) for its Cu(II) and Zn(II) complexes (Figs. 7 and 8).

## 4. Conclusions

Novel asymmetrical mesoporphyrinic compounds were synthesized by microwave assisted procedures in view of being used in biomedical applications. The compounds were characterized by elemental analysis, UV–Vis, FT-IR, NMR and EPR spectroscopy, which confirmed the proposed structures. UV–Vis spectra of the compounds in solvents with increasing polarity resulted in slight bathochromic shifts of both Soret and Q bands due to the specific interactions between the porphyrinic substituents and the solvent molecules.

Fluorescence emission quantum yields evaluated for all porphyrins under study, revealed high yields for the metal free compounds, followed by the zinc complex. The copper compounds are non-emissive or exhibit a reduced emission. A similar pattern was detected for singlet oxygen quantum yields of formation. These latter values are a good indication for their use as possible useful photosensitisers for photodynamic therapy. The newly mesoporphyrinic compounds have an optimistic toxicological profile, namely a lack of short term dark toxicity and only slight effect on the proliferative capacity of U937 cell line.

## Acknowledgements

The research was supported by MNT ERA NET projects No. 7-030/2010, 0003/2009 and 0004/2009 (FCT).

## References

[1] Detty MR, Gibson SL, Wagner SJ. Current clinical and Preclinical photosensitizers for use in photodynamic therapy. J Med Chem 2004;47:3897–915.
[2] Kamuhabwa A, Agostinis P, Ahmed B, Landuyt W, Van Cleynenbreugel B, Van Poppel H, et al. Ypericin as a potential phototherapeutic agent in superficial transitional cell carcinoma of the bladder. Photochem Photobiol Sci 2004;3:772–80.
[3] Hilderbrand S, Weissleder R. Near-infrared fluorescence: application to *in vivo* molecular imaging. Curr Opin Chem Biol 2010;14:71–9.
[4] Chatterjee DK, Yong Z. Nanoparticles in photodynamic therapy: an emerging paradigm. Adv Drug Deliv Rev 2008;60:1627–37.
[5] Bonneau S, .Bizet CV, Mojzisova H, Brault D. Tetrapyrrole-photosensitizers vectorization and plasma LDL: a physic-chemical approach. Int J Pharm 2007; 344:78–87.
[6] Chin WWL, O.Lau WK, Bhuvaneswari R, Heng PWS, Olivo M. Chlorin e6-polyvinylpyrrolidone as a fluorescent marker for fluorescence diagnosis of human bladder cancer implanted on the chick chorioallantoic membrane model. Cancer Lett 2007;245:127–33.
[7] Berg K, Selbo PK, Weyergang A, Dietze A, Prasmickaite L, Bonsted A. Porphyrin related photosensitizers for cancer imaging and therapeutic applications. J Microsc 2005;218:133–47.
[8] Ramaswamy B, Manivasager V, Chin WW, Soo KC, Olivo M. Photodynamic diagnosis of a human nasopharyngeal carcinoma xenograft model using the novel chlorin e6 photosensitizer fotolon. Int J Oncol 2005;26:1501–6.
[9] Sakamoto FH, Lopes JD, Anderson R. Photodynamic therapy for acne vulgaris: a critical review from basics to clinical practice. Part I. Acne vulgaris: when and why consider photodynamic therapy? J Am Acad Dermatol 2010;63: 183–93.
[10] Sakamoto FH, Torezan L, Anderson R. Photodynamic therapy for acne vulgaris: a critical review from basics to clinical practice Part II. Understanding parameters for acne treatment with photodynamic therapy. J Am Acad Dermatol 2010;63:195–211.
[11] de Oliveira Mima EG, Pavarina AC, Dovigo LN, Vergani CE, de Souza Costa CA, Kurachi C, et al. Susceptibility of *Candida albicans* to photodynamic therapy in a murine model of oral candidosis. Oral Surg Oral Med Oral Pathol Oral Radiol Endod 2010;109:392–401.
[12] Ragàs X, Agut M, Nonell S. Singlet oxygen in Escherichia coli: new insights for antimicrobial photodynamic therapy. Free Radic Biol Med 2010;49:770–6.
[13] Chin W, Lau W, Cheng C, Olivo M. Evaluation of hypocrellin B in a human bladder tumor model in experimental photodynamic therapy: biodistribution, light dose and drug-light interval effects. Int J Oncol 2004;25:623–9.
[14] Boscencu R, Socoteanu R, Ilie M, Sousa Oliveira A, Constantin C, Vieira Ferreira LF. Synthesis, spectral and biological evaluation of some mesoporphyrinic complexes of Zn(II). Revista De Chim 2009;60:1006–11.
[15] Boscencu R, Ilie M, Socoteanu R, Oliveira AS, Constantin C, Neagu M, et al. Microwave synthesis, basic spectral and biological evaluation of some copper (II) mesoporphyrinic complexes. Molecules 2010;15:3731–43.
[16] Boscencu R, Socoteanu R, Oliveira AS, Vieira Ferreira LF, Nacea V, Patrinoiu G. Synthesis and characterisation of some new unsymmetrically-substituted mesoporphyrinic mono-hydroxyphenyl complexes of Cu(II). Polish J Chem 2008;82:509–21.
[17] Boscencu R, Socoteanu R, .Oliveira AS, Vieira Ferreira LF. Studies on Zn(II) Monohydroxyphenyl substituted mesoporphyrins synthesis and characterisation. J Serbian Chem Soc 2008;73:713–26.
[18] Boscencu R, Licsandru D, Socoteanu R, Oliveira A, Vieira Ferreira LF. Synthesis and spectral characterisation of some unsymmetrically substituted mesoporphyrinic compounds. Revista De Chim 2007;58:498–502.
[19] Jori G, Schind L, Schind A, Polo L. Novel approaches towards a detailed control of the mechanism and efficiency of photosensitized processes in vivo. J Photochem Photobiol A: Chem 1996;102:101–7.
[20] Stolik S, Delgado JA, Pérez A, Anasagasti L. Measurement of the penetration depths of red and near infrared light in human "ex vivo" tissues. J Photochem Photobiol B 2000;57:90–3.
[21] Boyle RW, Dolphin D. Structure and biodistribution relationships of photodynamic sensitizers. Photochem Photobiol 1996;64:469–85.
[22] Pascu S, Waghorn P, Conry T, Lin B, James C, Zayed JM. Design considerations towards simultaneously radiolabeled and fluorescent imaging probes incorporating metallic species. Adv Inorg Chem 2009;61:131–78.
[23] Ricchelli F, Jori G, Gobbo S, Tronchin M. Liposomes as models to study the distribution of porphyrins in cell membranes. Biochim Biophys Acta 1991; 1065:42–8.
[24] Milanesio ME, Alvarez MG, Silber JJ, Rivarola V, Durantini EN. Photodynamic activity of monocationic and no-charged methoxyphenylporphyrin derivatives in homogeneous and biological media. Photochem Photobiol Sci 2003;2:926–33.
[25] Riccheli F, Franchi L, Miotto G, Borsetto L, Gobbo S, .Nicolov P, et al. Meso-substituted tetra-cationic porphyrins photosensitize the death of human fibrosarcoma cells via lysosomal targeting. Int J Biochem Cell Biol 2005;37: 306–19.
[26] Riccheli F. Photophysical properties of porphyrins in biological membranes. J Photochem Photobiol B: Biol 1995;29:109–18.
[27] Zhenyu J, Yang G, Vasovic V, Cunderlikova B, Suo Z, Nesland JM, et al. Subcellular localization pattern of protoporphyrin IX is an important determinant for its photodynamic efficiency of human carcinoma and normal cell lines. J Photochem Photobiol B Biol 2006;84:213–20.

[28] Socoteanu R, Boscencu R, Nacea V, Oliveira AS, Vieira Ferreira LF. Microwave-assisted synthesis of unsymmetrical tetrapyrrolic compounds. Revista De Chim 2008;59:969–72.
[29] Korzeniewski C, Callewaert DM. An enzyme-release assay for natural cytotoxicity. J Immunol Meth 1983;64:313–20.
[30] Barltrop JA, Owen TC, Cory AH, Cory JG. 5-(3-carboxymethoxyphenyl)-2-(4,5-dimethylthiazolyl)-3-(4-sulfophenyl)tetrazolium, inner salt (MTS) and related analogs of 3-(4,5-dimethylthiazolyl)-2,5-diphenyltetrazolium bromide (MTT) reducing to purple water-soluble formazans as cell-viability indicators. Bioorg Med Chem Lett 1991;1:611–4.
[31] Branco TJF, Botelho do Rego AM, Ferreira Machado I, Vieira Ferreira LF. A luminescence lifetime distributions analysis in heterogeneous systems by the use of Excel's Solver. J Phys Chem B 2005;109:15958–67.
[32] Botelho do Rego AM, Vieira Ferreira LF. Photonic and electronic spectroscopies for the characterization of organic surfaces and organic molecules adsorbed on surfaces. In: Nalwa HS, editor. Handbook of surfaces and interfaces of materials. Academic Press; 2001. p. 275–313.
[33] Lin WC. Electron spin resonance and electronic structure of metalloporphyrins. In: Dolphin D, editor. The porphyrins. New York, NY, USA: Academic Press; 1978. p. 358.
[34] Manoharan PT, Roger MT. In: Yen TF, editor. Electron spin resonance of metal complexes. New York, NY, USA: Plenum Press; 1969. p. 143.
[35] Kivelson D, Neiman RR. ESR studies on the bonding in copper complexes. J Chem Phys 1961;35:149–55.
[36] Gouterman M. Optical spectra and electronic structure of porphyrins and related rings. In: Dolphin D, editor. The porphyrins. New York: Academic Press; 1978. p. 1–165.
[37] Rendel D. Fluorescence and posphorescence spectroscopy. John Wiley and Sons; 1987.
[38] Rechmond RW, Braslavsky SE. NATO ASI Ser. Ser H 1988;15:93–5.
[39] Gouterman M, Khalil GE. Porphyrin free base phosphorescence. J Mol Spectrosc 1974;53:88–100.
[40] Milgrom LR. The colours of life. Oxford University Press; 1997.
[41] Brown SB, Brown EA, Walker I. The present and future role of photodynamic therapy in cancer treatment. Lancet Oncol 2004;5:497–508.
[42] Allison RR, Sibata CH. Oncologic photodynamic therapy photosensitizers: a clinical review. Photodiagnosis Photodyn Ther 2010;7:61–75.
[43] Pandey RK, Goswami LN, Chen Y, Gryshuk A, Missert JR, Oseroff A, et al. Nature: a rich source for developing multifunctional agents. Tumor-imaging and photodynamic therapy. Lasers Surg Med 2006;38:445–67.